

Monitoring statistics of the ERS-2 scatterometer for ESA

Cycle 153

(Project Ref. 22025/08/I-EC)

Hans Hersbach
European Centre for Medium-Range Weather Forecasts,
Shinfield Park, Reading, RG2 9AX, England
Tel: (+44 118) 9499476, e-mail: dal@ecmwf.int

January 21, 2010

1 Introduction

The quality of the UWI product was monitored at ECMWF for Cycle 153. Results were compared to those obtained from the previous Cycle, as well for data received during the nominal period in 2000 (up to Cycle 59). No corrections for duplicate observations from overlapping ground stations were applied.

During Cycle 153 data was received between 21:07 UTC 7 December 2009 and 21:00 UTC 11 January 2010. Data was grouped into 6-hourly batches (centred around 00, 06, 12 and 18 UTC). No data was received for the batches for 06 UTC and 18 UTC on 13 December 2009, for 06 UTC 28 December 2009, and from 6 UTC 2 January 2010 to 18 UTC 3 January 2010.

Data is being recorded whenever within the visibility range of a ground station. For Cycle 153, data coverage was over the North-Atlantic, part of the Mediterranean, the Gulf of Mexico, a very small part of the Pacific west from the US, Canada and Central America, the Chinese Sea, a small part of the Indian Ocean south-east from Thailand and Indonesia, and an area near Antarctica and south from Australia (see Figure 2).

Time series of the asymmetry between the fore and aft incidence angles show, besides a rather large peak on 9 December 2009, a reasonably calm behaviour.

Compared to Cycle 152, the UWI wind speed relative to ECMWF first-guess (FG) fields showed a higher standard deviation (1.59 m/s, was 1.54 m/s). Bias levels were slightly less negative (on average -0.83 m/s, was -0.86 m/s).

Ocean calibration shows that the small inter-node and inter-beam dependencies of bias levels as observed during Cycle 152, were retained. Average bias levels were less negative

(-0.42 dB, was -0.51 dB; see Figure 4).

The ECMWF operational assimilation was not changed during Cycle 153.

The Cycle-averaged evolution of performance relative to ECMWF first-guess (FG) winds is displayed in Figure 1. Figure 2 shows global maps of the over Cycle 153 averaged UWI data coverage and wind climate, Figure 3 for performance relative to FG winds.

2 ERS-2 statistics from 7 December 2009 to 11 January 2010

2.1 Sigma0 bias levels

The average sigma0 bias levels (compared to simulated sigma0's based on ECMWF model FG winds) stratified with respect to antenna beam, ascending or descending track and as function of incidence angle (i.e. across-node number) is displayed in Figure 4.

Compared to Cycle 152, inter-node and inter-beam dependencies between the fore and aft antenna remain small. Average bias level was less negative (-0.42 dB, was -0.51 dB), being on the level of nominal data in 2000 (around -0.4 dB; see Figure 1 of the reports for Cycle 48 to 59). The situation is better than that of one year ago (see report for Cycle 143).

Long-term variations correlate with the yearly cycle, which, given the non-global coverage, is understandable. Therefore, the method of ocean calibration will probably only provide accurate information on calibration levels for globally or yearly averaged data sets.

The data volume of descending tracks was about 29% lower than for ascending tracks.

2.2 Incidence angles

For ESACA, across-node binning is, like the old processor, retained on a 25km mesh. From simple geometrical arguments it follows that variations in yaw attitude will lead to asymmetries between the incidence angles of the fore and aft beam. Indeed, this has been observed. Figure 5 gives a time evolution of this asymmetry. Also in this Figure, the occasions for which the combined k_p -yaw quality flag was set are indicated by red stars. The relation with incidence-angle asymmetries is obvious.

The asymmetry between the fore and aft incidence angles was relatively calm. Although, a rather large peak did occur on 9 December 2009. Around 13 and 14 December 2009 the Geomid meteor shower reached an intense maximum. It didn't seem to affect the ERS2 attitude control. From mid December onwards several large sun spots emerged, which may mark the end of the deepest solar minimum in 100 years. Associated eruptions did not affect the Earth magnetic field, though (source: www.spaceweather.com).

2.3 Distance to cone history

The distance to the cone history is shown in Figure 6. Curves are based on data that passed all QC, including the test on the k_p -yaw flag, and subject to the land and sea-ice check at ECMWF (see cyclic report 88 for details).

Like for previous Cycles, time series are (due to lack of statistics) very noisy, especially for the near-range nodes. Most spikes were found to be the result of low data volumes.

Compared to Cycle 152, the average level has improved (1.18 was 1.22), and is higher (by 8%) than for nominal data (see top panel Figure 1).

The fraction of data that did not pass QC is displayed in Figure 6 as well (dashed curves).

2.4 UWI minus First-Guess wind history

In Figure 7, the UWI minus ECMWF first-guess wind-speed history is plotted. The history plot shows a few peaks, which are usually the result of low data volume.

Figure 11 displays the locations for which UWI winds were more than 8 m/s weaker (top panel), respectively more than 8 m/s stronger (lower panel) than FG winds. Like for Cycle 152, such collocations are isolated, and often indicate meteorologically active regions, for which UWI data and ECMWF model field show reasonably small differences in phase and/or intensity. Deviations near the poles are the result of imperfect sea-ice flagging.

Two cases for which UWI winds were considerably different from FG winds are presented in Figure 12. The top panel displays a rather complex system in the North Atlantic for 13 December 2009. The UWI product indicates much sharper gradients in wind directions. The lower panel displays a clearly degraded UWI product in the Hudson Bay for 15 December 2009. From the OSI SAF sea-ice product, on which the ECMWF sea-ice analysis relies, it emerges that this part of the Hudson Bay froze over quickly that day (not shown). This most likely explains the incorrect flagging for the degraded part of the UWI swath.

Average bias levels and standard deviations of UWI winds relative to FG winds are displayed in Table 1. From this it follows that the bias of UWI winds was slightly less negative (-0.83 m/s, was -0.86 m/s), being around the level of nominal data in 2000.

On a longer time scale seasonal bias trends are observed (see Figure 1). The large increase in negative bias that had emerged several Cycles ago, and its current reduction are typical for this season. As was highlighted in previous cyclic reports, it is believed that this yearly trend is partly induced by changing local geophysical conditions.

The standard deviation of UWI wind speed versus ECMWF FG has, compared to Cycle 152, increased (1.59 m/s, was 1.54 m/s).

For Cycle 153 the (UWI - FG) direction standard deviations were mostly ranging between 20 and 40 degrees (Figure 8). Average STDV for UWI wind direction has somewhat increased compared to that of Cycle 152 (30.2 degrees, was 29.7 degrees). For at ECMWF de-aliased winds (Figure 10) performance appeared slightly improved (STDV 19.4, was 19.8 degrees).

	Cycle 152		Cycle 153	
	UWI	CMOD4	UWI	CMOD4
speed STDV	1.54	1.53	1.59	1.58
node 1-2	1.59	1.55	1.58	1.55
node 3-4	1.48	1.46	1.51	1.50
node 5-7	1.43	1.43	1.51	1.51
node 8-10	1.48	1.47	1.53	1.54
node 11-14	1.53	1.53	1.56	1.57
node 15-19	1.53	1.55	1.61	1.62
speed BIAS	-0.86	-0.85	-0.83	-0.82
node 1-2	-1.49	-1.46	-1.49	-1.46
node 3-4	-1.21	-1.15	-1.18	-1.13
node 5-7	-0.91	-0.87	-0.86	-0.82
node 8-10	-0.68	-0.67	-0.64	-0.63
node 11-14	-0.61	-0.62	-0.59	-0.60
node 15-19	-0.64	-0.65	-0.61	-0.63
direction STDV	29.7	19.8	30.2	19.4
direction BIAS	-2.6	-3.0	-1.8	-2.1

Table 1: Biases and standard deviation of ERS-2 versus ECMWF FG winds in m/s for speed and degrees for direction.

2.5 Scatterplots

Scatterplots of FG winds versus ERS-2 winds are displayed in Figures 13 to 16. Values of standard deviations and biases are slightly different from those displayed in Table 1. Reason for this is that, for plotting purposes, the in 0.5 m/s resolution ERS-2 winds have been slightly perturbed (increases scatter with 0.02 m/s), and that zero wind-speed ERS-2 winds have been excluded (decreases scatter by about 0.05 m/s).

The scatterplot of UWI wind speed versus FG (Figure 13) is very similar to that for (at ECMWF inverted) de-aliased CMOD4 winds (Figure 15). It confirms that the ESACA inversion scheme is working properly.

Winds derived on the basis of CMOD5 are displayed in Figure 16. The relative standard deviation is lower than for CMOD4 winds (1.54 m/s versus 1.61 m/s). Compared to ECMWF FG, CMOD5 winds are 0.31 m/s slower.

Figure Captions

Figure 1: Evolution of the performance of the ERS-2 scatterometer averaged over 5-weekly Cycles from 12 December 2001 (Cycle 69) to 11 January 2010 (end Cycle 153) for the UWI product (solid, star) and de-aliased winds based on CMOD4 (dashed, diamond). Results are based on data that passed the UWI QC flags. For Cycle 85 two values are plotted; the first value for a global set, the second one for a regional set (for details see

the corresponding cyclic report). Dotted lines represent values for Cycle 59 (5 December 2000 to 17 January 2001), i.e. the last stable Cycle of the nominal period. From top to bottom panel are shown the normalized distance to the cone (CMOD4 only) the standard deviation of the wind speed compared to FG winds, the corresponding bias (for UWI winds the extremes in node-wise averages are shown as well), and the standard deviation of wind direction compared to FG.

Figure 2: Average number of observations per 12H and per 125km grid box (top panel) and wind climate (lower panel) for UWI winds that passed the UWI flags QC and a check on the collocated ECMWF land and sea-ice mask.

Figure 3: The same as Figure 2, but now for the relative bias (top panel) and standard deviation (lower panel) with ECMWF first-guess winds.

Figure 4: Ratio of $\langle \sigma_0^{0.625} \rangle / \langle \text{CMOD4}(\text{FirstGuess})^{0.625} \rangle$ converted in dB for the fore beam (solid line), mid beam (dashed line) and aft beam (dotted line), as a function of incidence angle for descending and ascending tracks. The thin lines indicate the error bars on the estimated mean. First-guess winds are based on the in time closest (+3h, +6h, +9h, or +12h) T799 forecast field, and are bilinearly interpolated in space.

Figure 5: Time series of the difference in incidence angle between the fore and aft beam. Red stars indicate the occurrences for which the combined k_p -yaw flag was set.

Figure 6: Mean normalized distance to the cone computed every 6 hours for nodes 1-2, 3-4, 5-7, 8-10, 11-14 and 15-19). The dotted curve shows the number of incoming triplets in logarithmic scale (1 corresponds to 60,000 triplets) and the dashed one indicates the fraction of complete (based on the land and sea-ice mask at ECMWF) sea-located triplets rejected by ESA flags, or by the wind inversion algorithm (0: all data kept, 1: no data kept).

Figure 7: Mean (solid line) and standard deviation (dashed line) of the wind speed difference UWI - first guess for the data retained by the quality control.

Figure 8: Same as Fig. 7, but for the wind direction difference. Statistics are computed for winds stronger than 4 m/s.

Figures 9 and 10: Same as Fig. 7 and 8 respectively, but for the de-aliased CMOD4 data.

Figure 11: Locations of data during Cycle 153 for which UWI winds are more than 8 m/s weaker (top panel) respectively stronger (lower panel) than FG, and on which QC on UWI flags and the ECMWF land/sea-ice mask was applied.

Figure 12: Comparison of UWI winds (in red) with ECMWF FG winds (in blue) for a case on 13 December 2009 (top panel) in the North Atlantic and a case on 15 December 2009 (lower panel) in the Hudson Bay.

Figure 13: Two-dimensional histogram of first guess and UWI wind speeds, for the data kept by the UWI flags, and QC based on the ECMWF land and sea-ice mask. Circles denote the mean values in the y-direction, and squares those in the x-direction.

Figure 14: Same as Fig. 13, but for wind direction. Only winds stronger than 4m/s are taken into account.

Figure 15: Same as Fig. 13, but for de-aliased CMOD4 winds.

Figure 16: Same as Fig. 13, but for de-aliased CMOD5 winds.

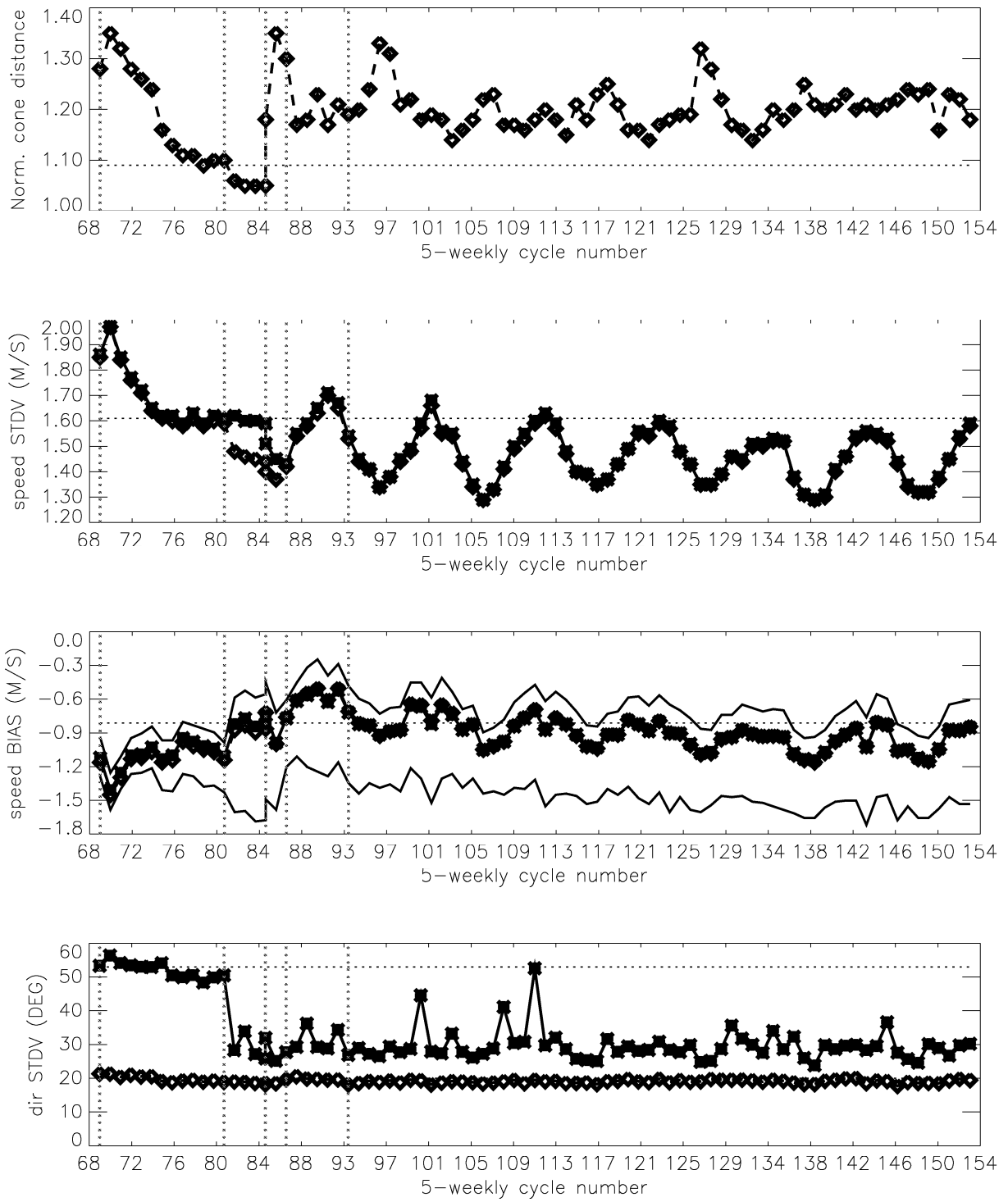
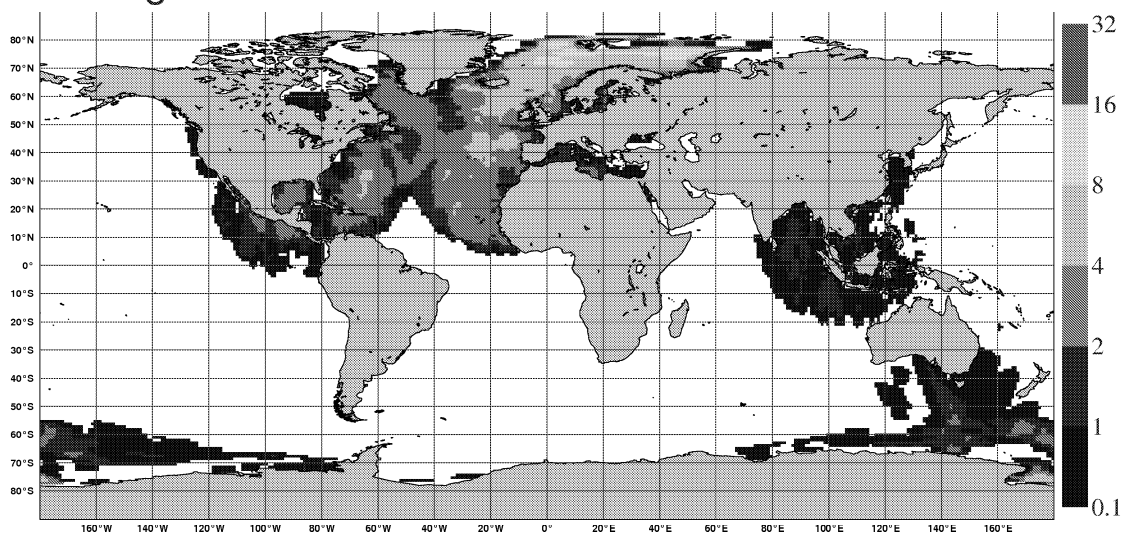


Figure 1

NOBS (ERS-2 UWI), per 12H, per 125km box
average from 2009120800 to 2010011118 GLOB:1.57



AVERAGE (ERS-2 UWI), in m/s.
average from 2009120800 to 2010011118 GLOB:6.82

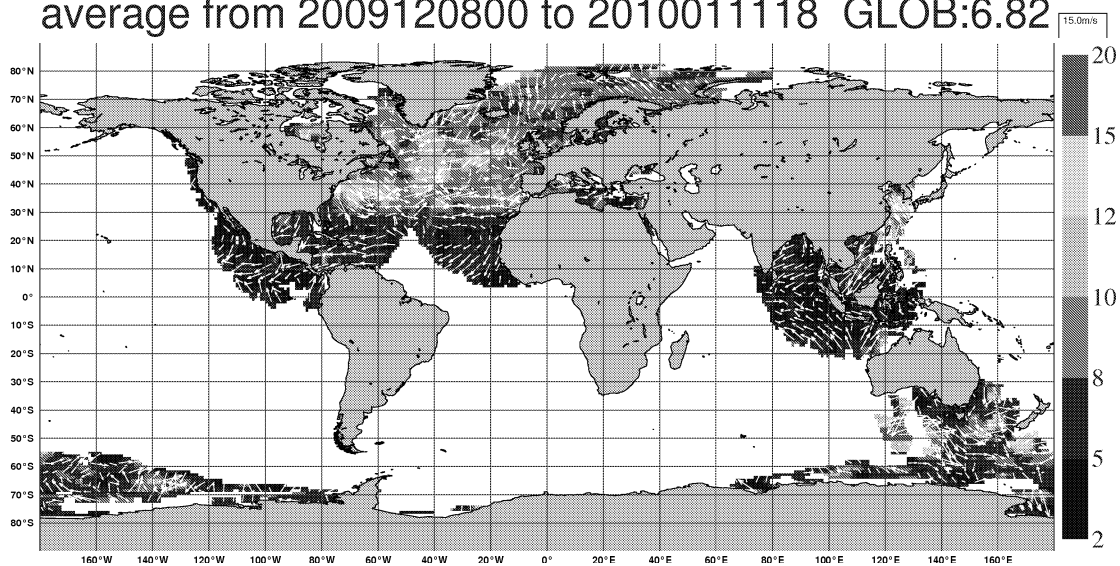
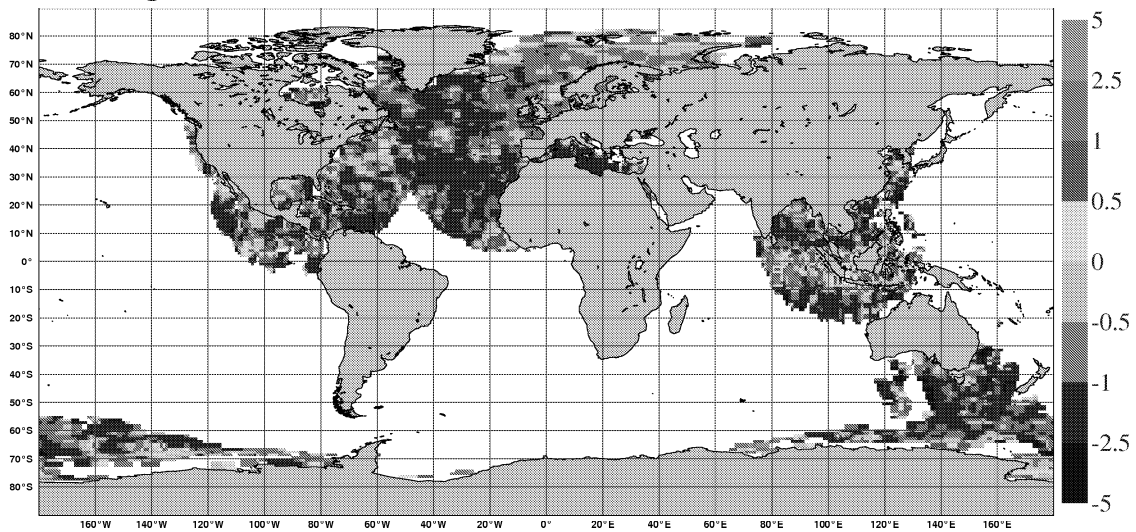


Figure 2

BIAS (ERS-2 UWI vs FIRST-GUESS), in m/s.
average from 2009120800 to 2010011118 GLOB:-0.81



STDV (ERS-2 UWI vs FIRST-GUESS), in m/s.
average from 2009120800 to 2010011118 GLOB:1.17

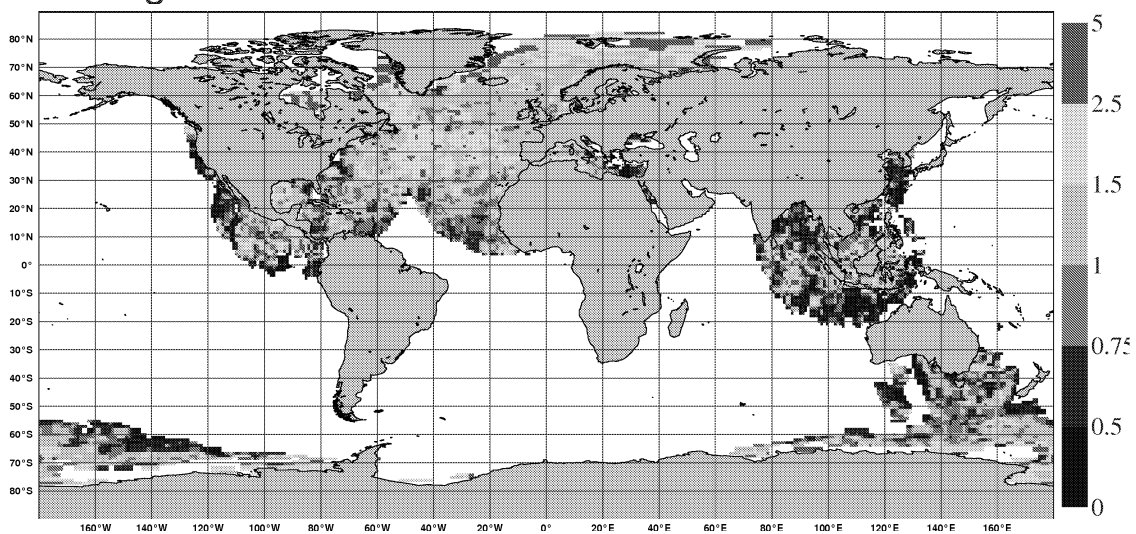


Figure 3

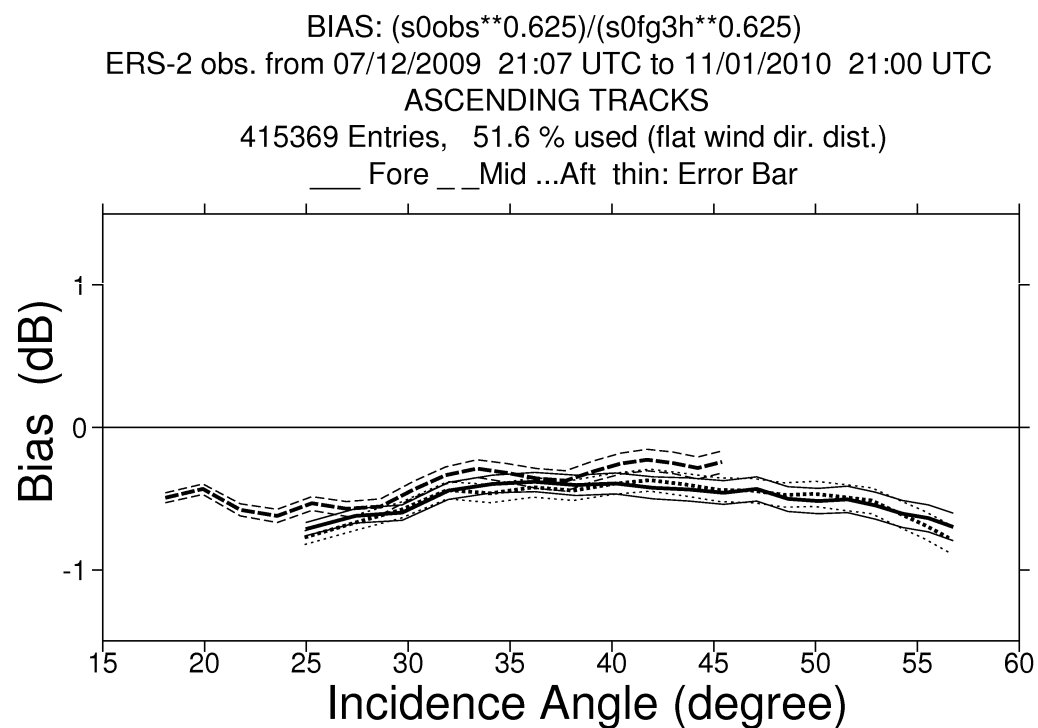
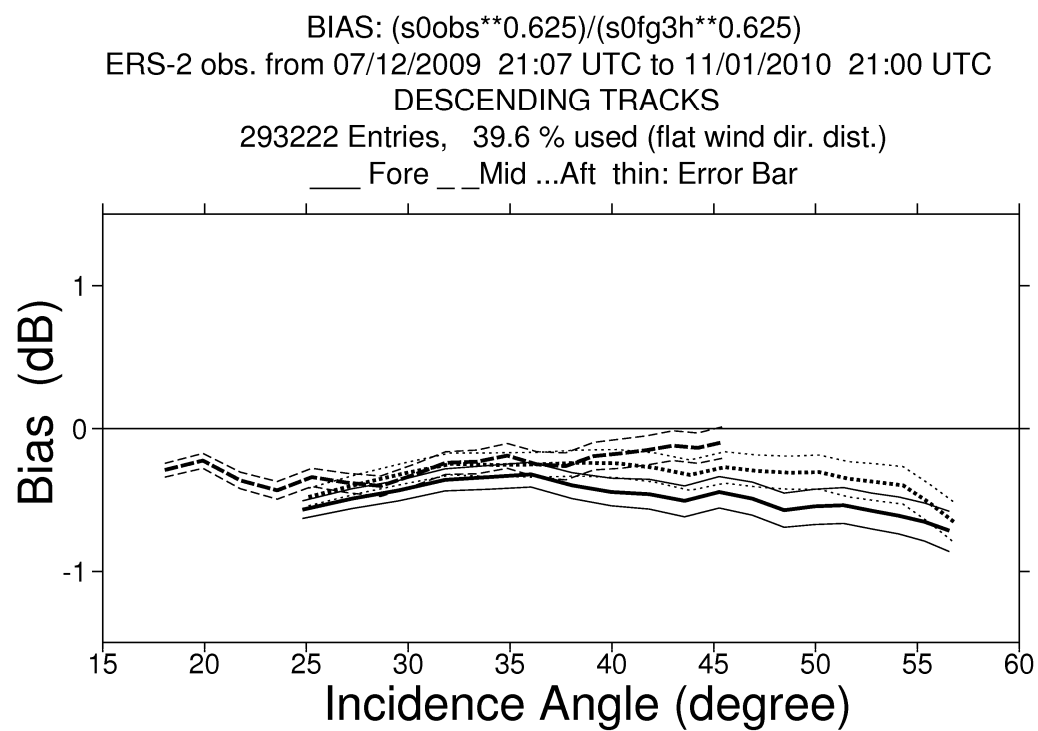


Figure 4

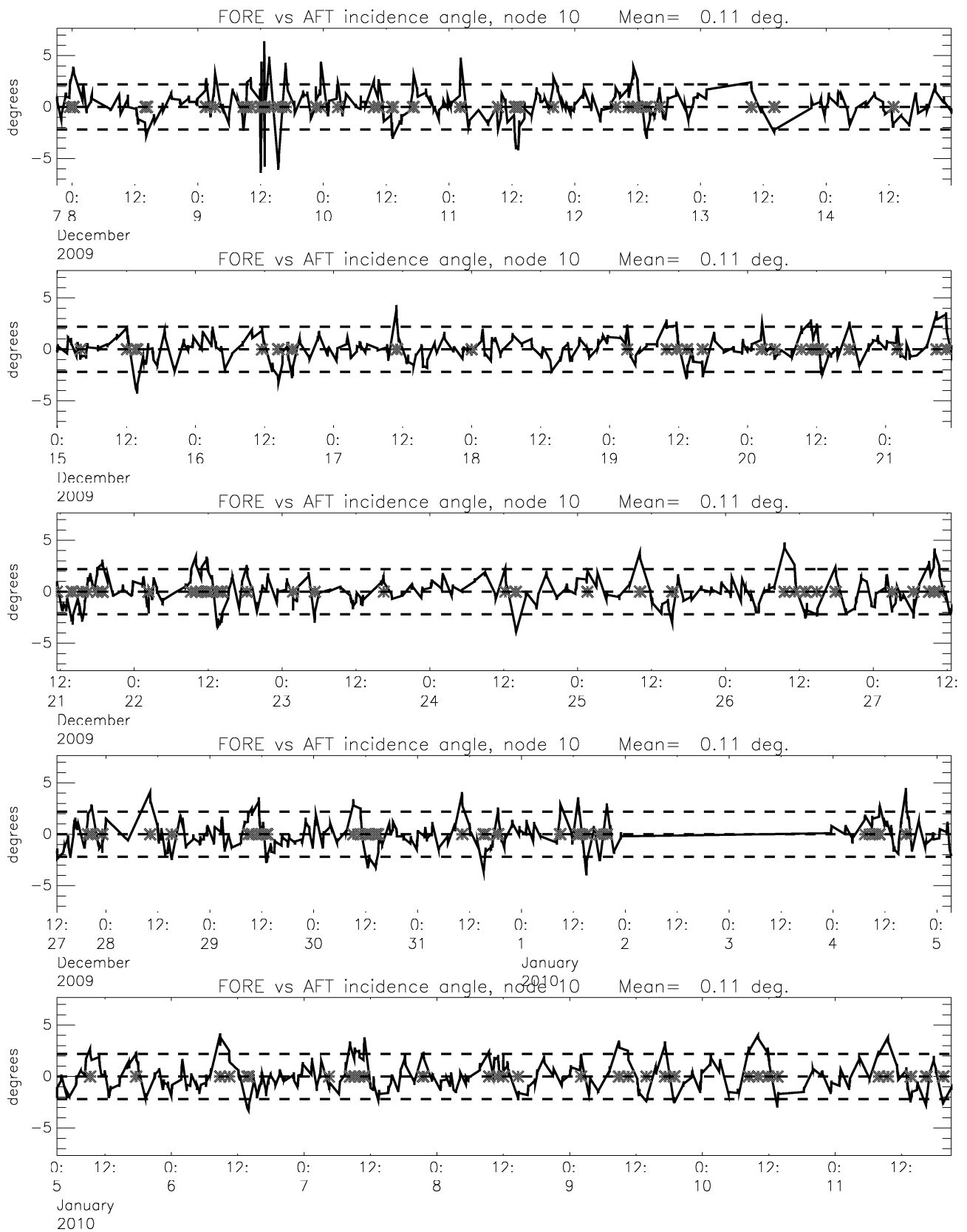


Figure 5

Monitoring of Sigma0 triplets versus CMOD4 for ERS-2

from 2009120800 to 2010011118

(solid) mean normalised distance to the cone over 6 h

(dashed) fraction of complete sea-point observations rejected by ESA flag or CMOD4 inversion

(dotted) total number of data in log. scale (1 for 60000)

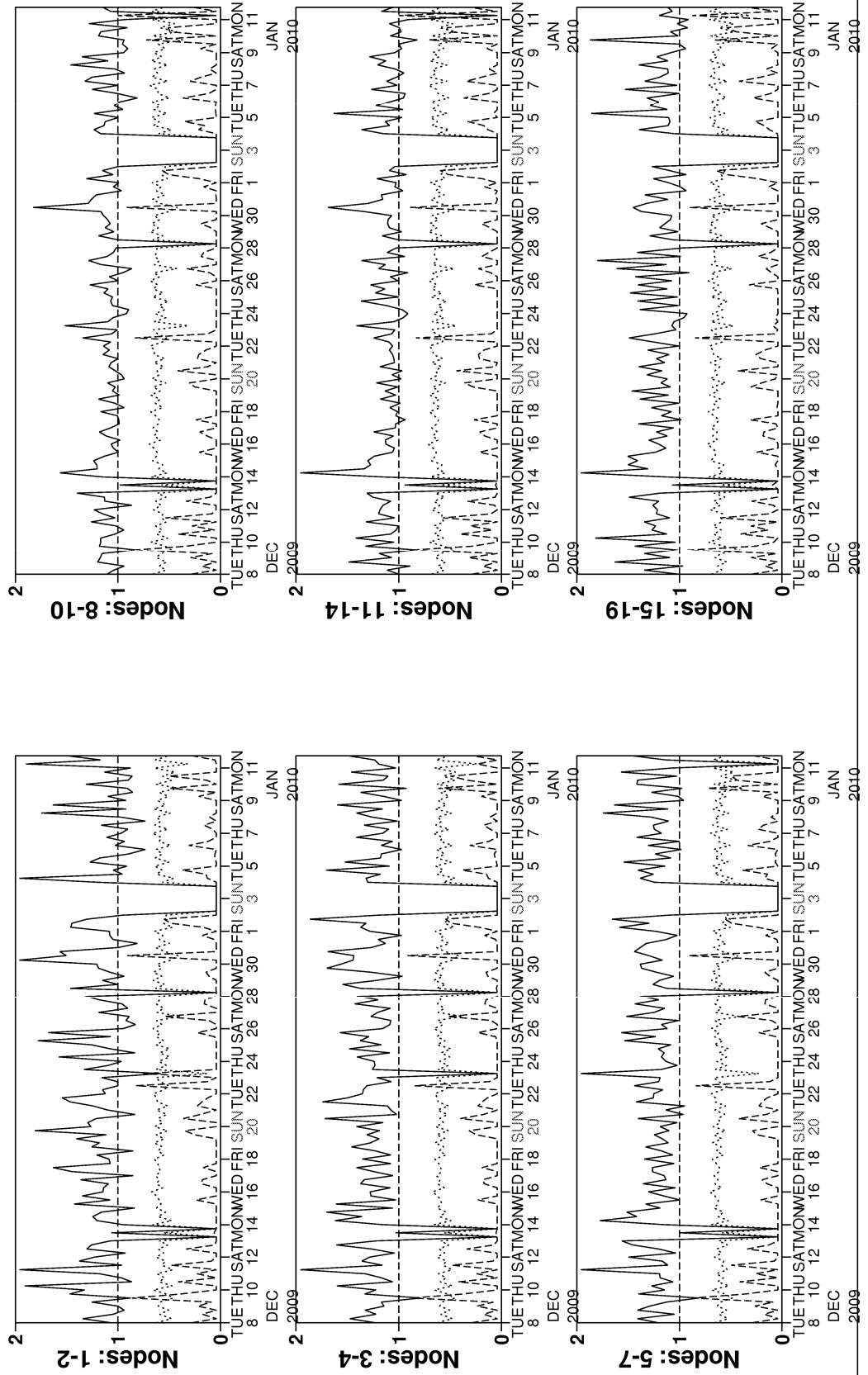


Figure 6

Monitoring of UWI winds versus First Guess for ERS-2

from 2009120800 to 2010011118

(solid) wind speed bias UWI - First Guess over 6h (deg.)
(dashed) wind speed standard deviation UWI - First Guess over 6h (deg.)

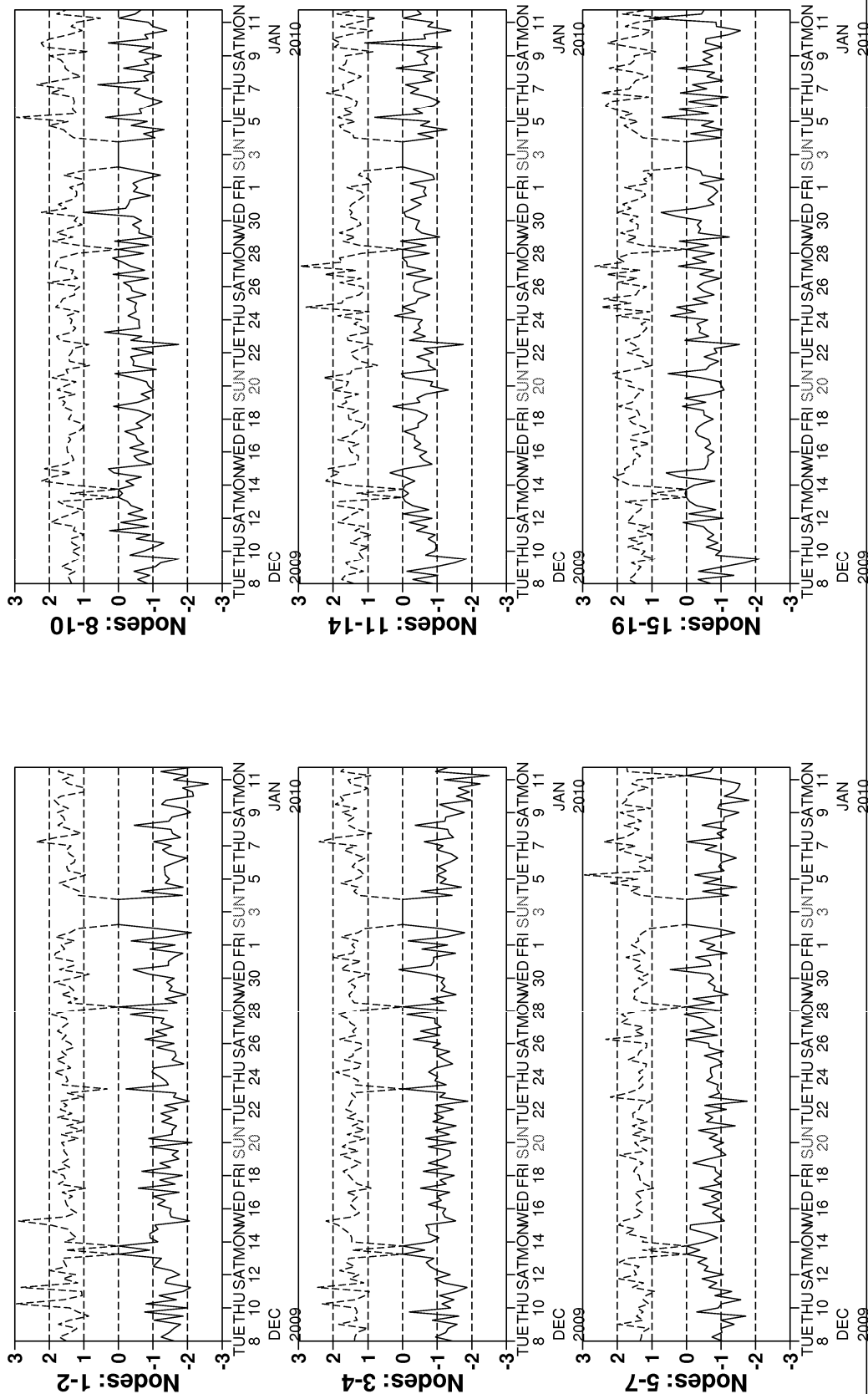


Figure 7

Monitoring of UWI winds versus First Guess for ERS-2

from 2009120800 to 2010011118

(solid) wind direction bias UWI - First Guess over 6h (deg.)

(dashed) wind direction standard deviation UWI - First Guess over 6h (deg.)

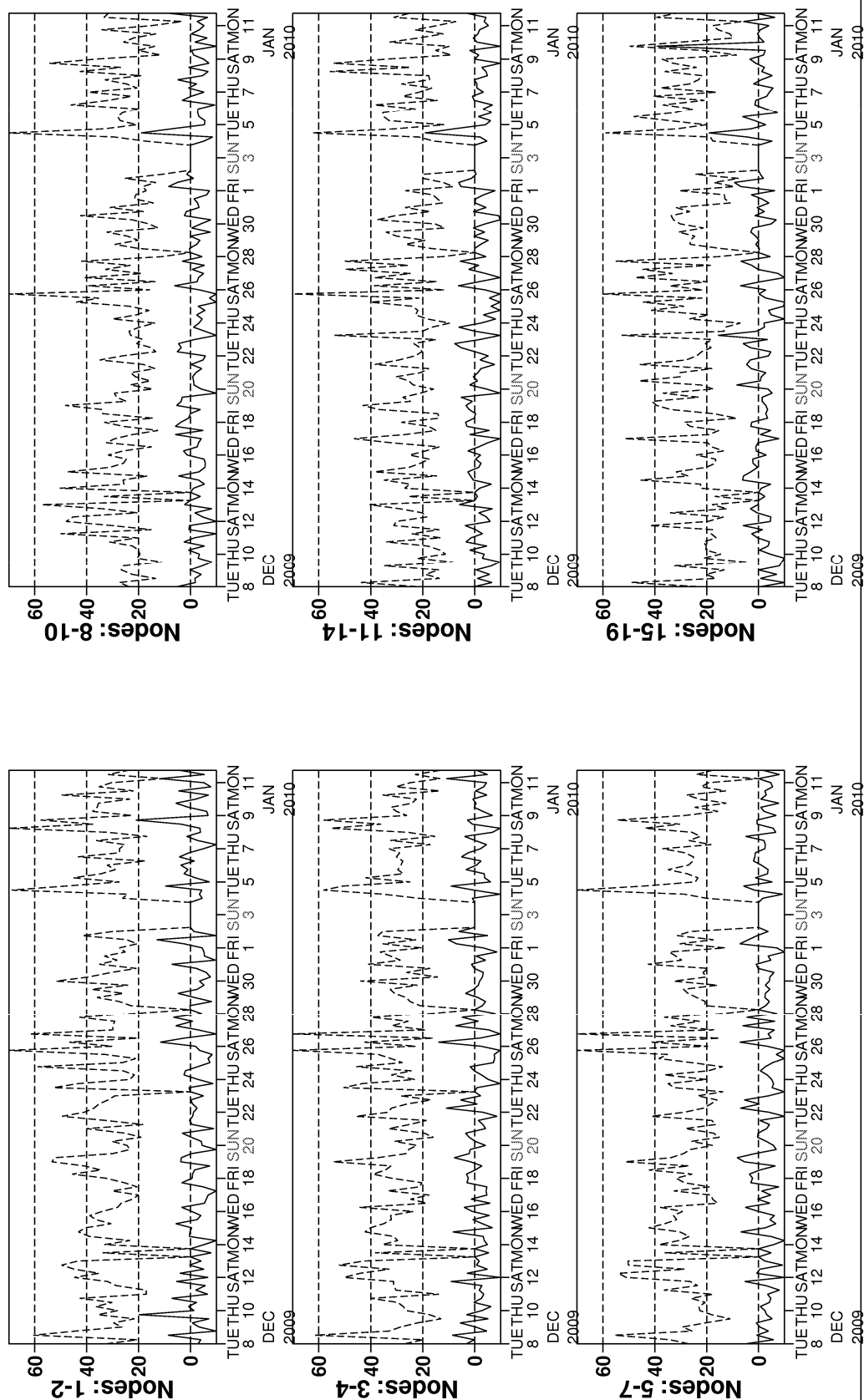


Figure 8

Monitoring of de-aliased CMOD4 winds versus First Guess for ERS-2

from 2009120800 to 2010011118

(solid) wind speed bias CMOD4 - First Guess over 6h (deg.)

(dashed) wind speed standard deviation CMOD4 - First Guess over 6h (deg.)

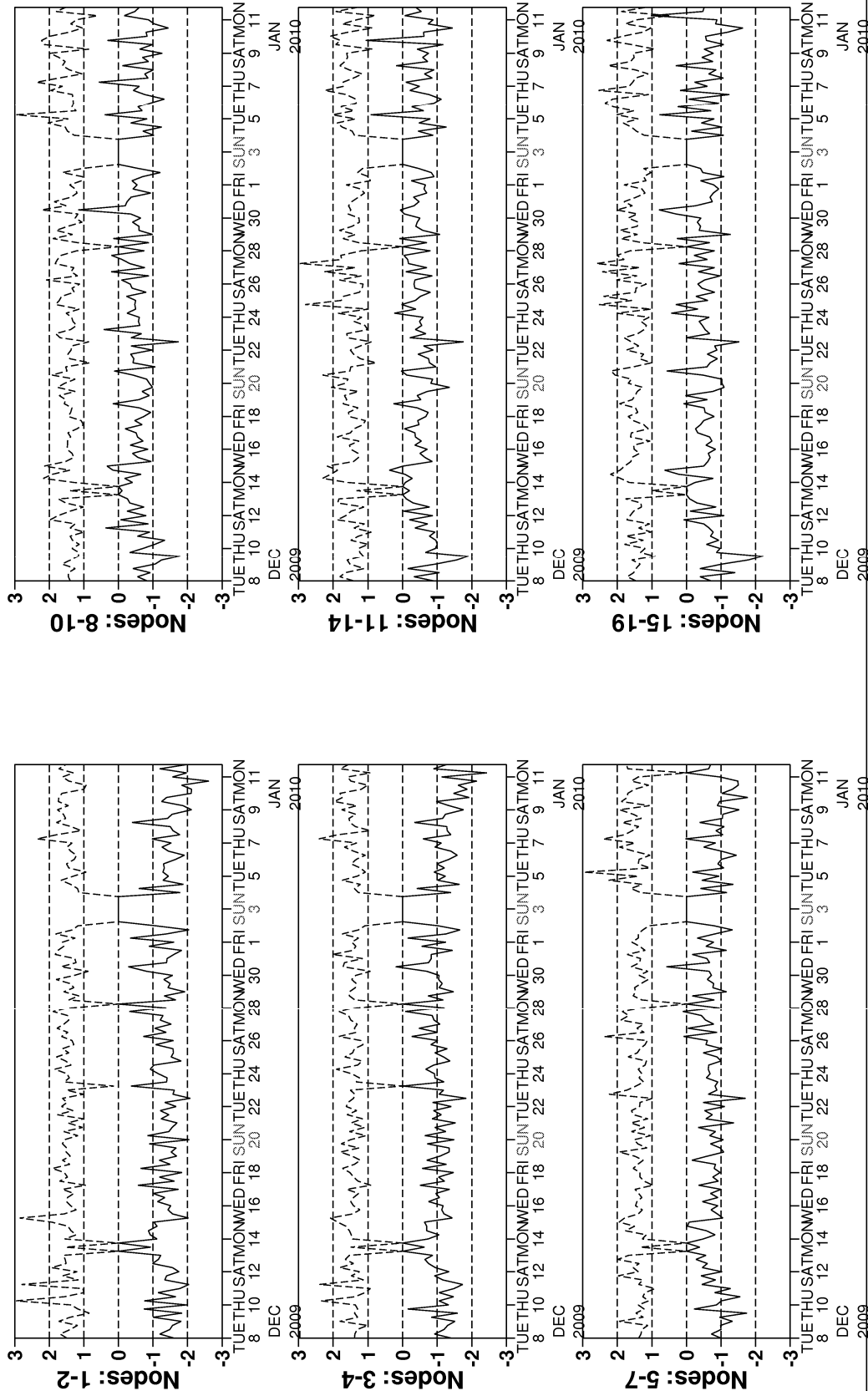


Figure 9

from 2009120800 to 2010011118

(solid) wind direction bias CMOD4 - First Guess over 6h (deg.)

(dashed) wind direction standard deviation CMOD4 - First Guess over 6h (deg.)

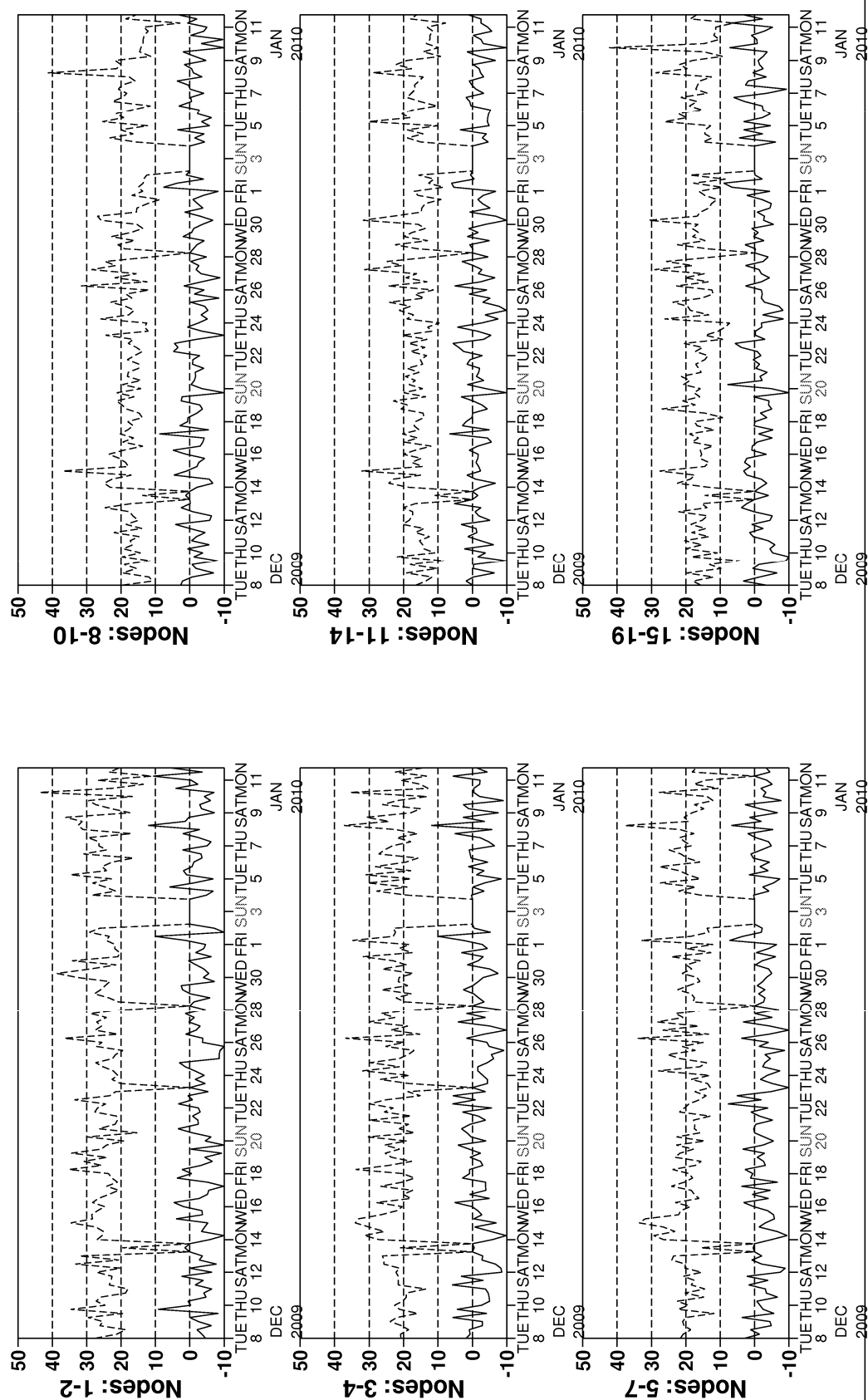
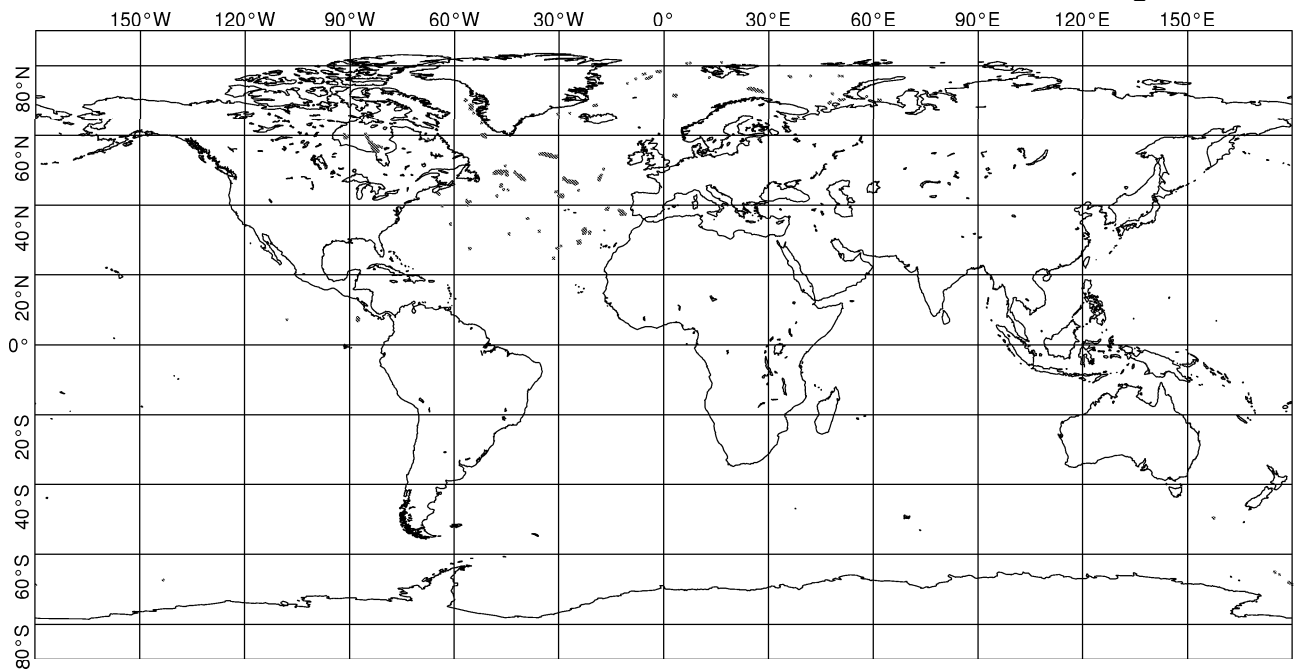


Figure 10

UWI winds more than 8 m/s weaker than ECMWF First Guess
CYCLE 153, 2009120800 to 2010011118, QC on ESA flags



UWI winds more than 8 m/s stronger than ECMWF First Guess
CYCLE 153, 2009120800 to 2010011118, QC on ESA flags

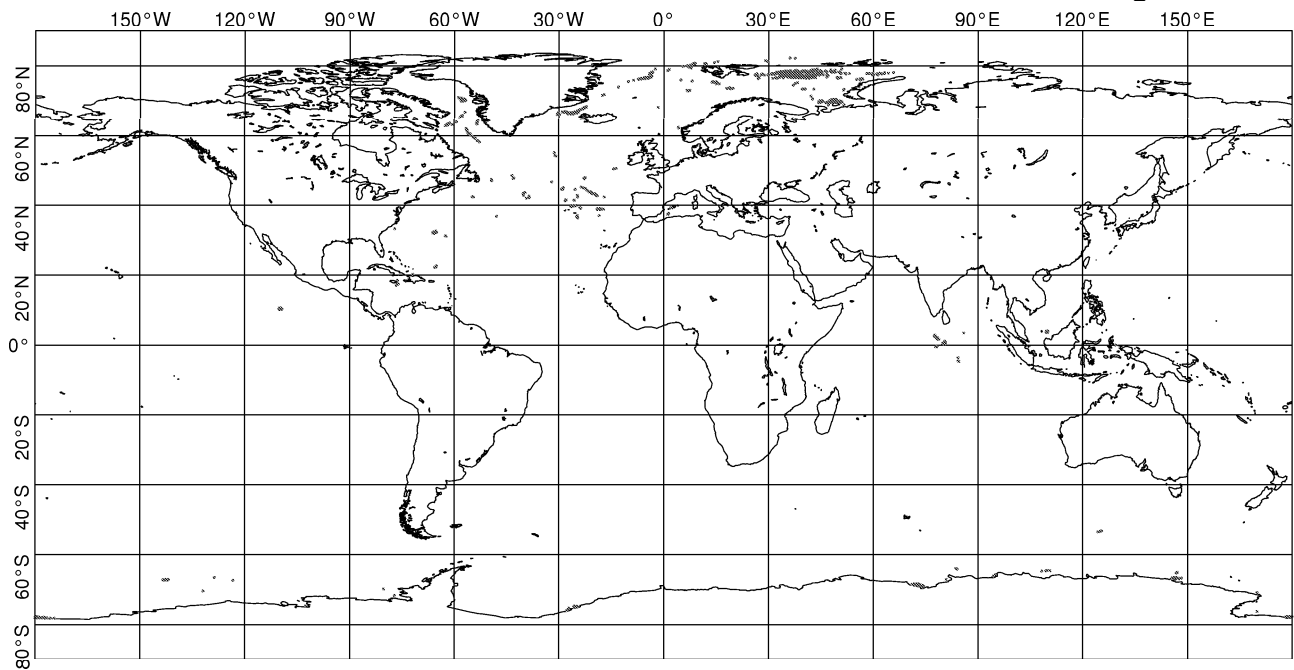
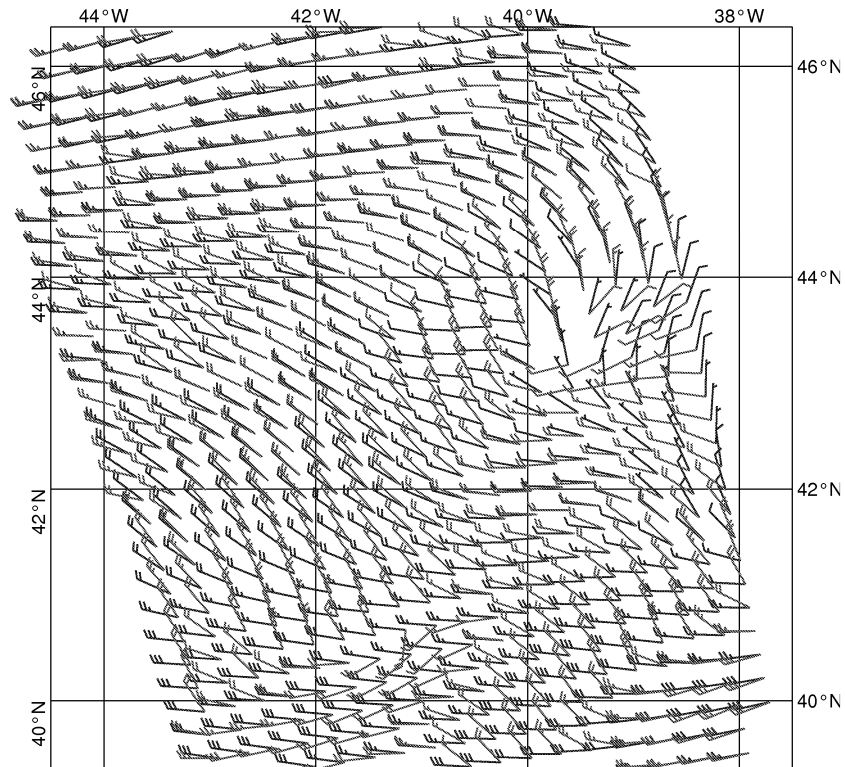


Figure 11

UWI winds (red) versus ECMWF FG winds (blue)
North Atlantic 20091213 01:05 UTC



UWI winds (red) versus ECMWF FG winds (blue)
Hudson Bay 20091215 03:27 UTC

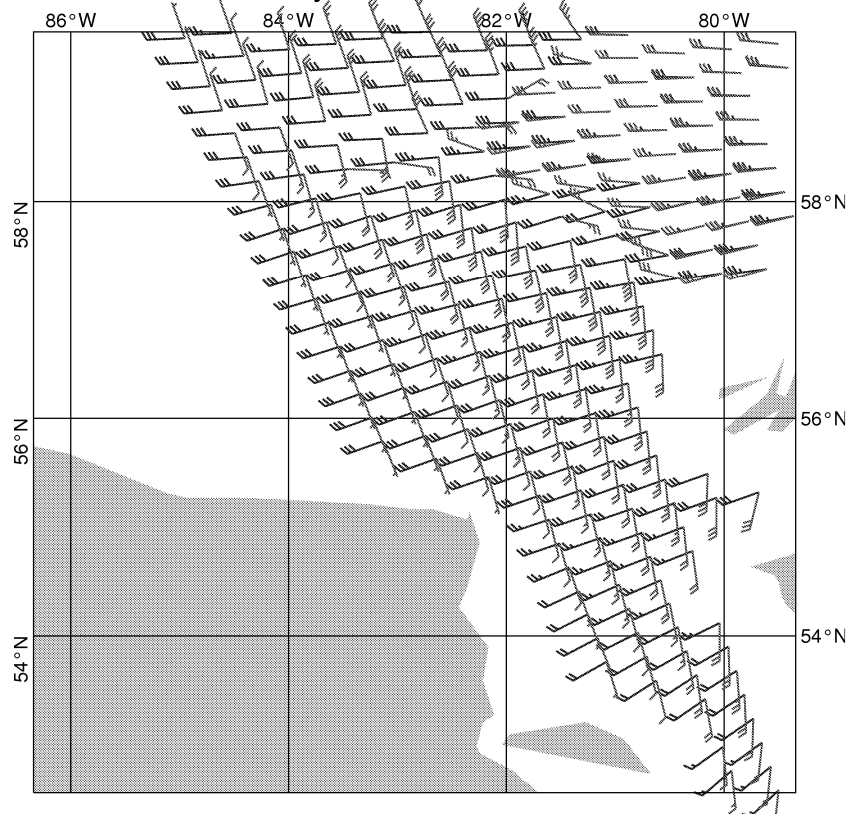


Figure 12

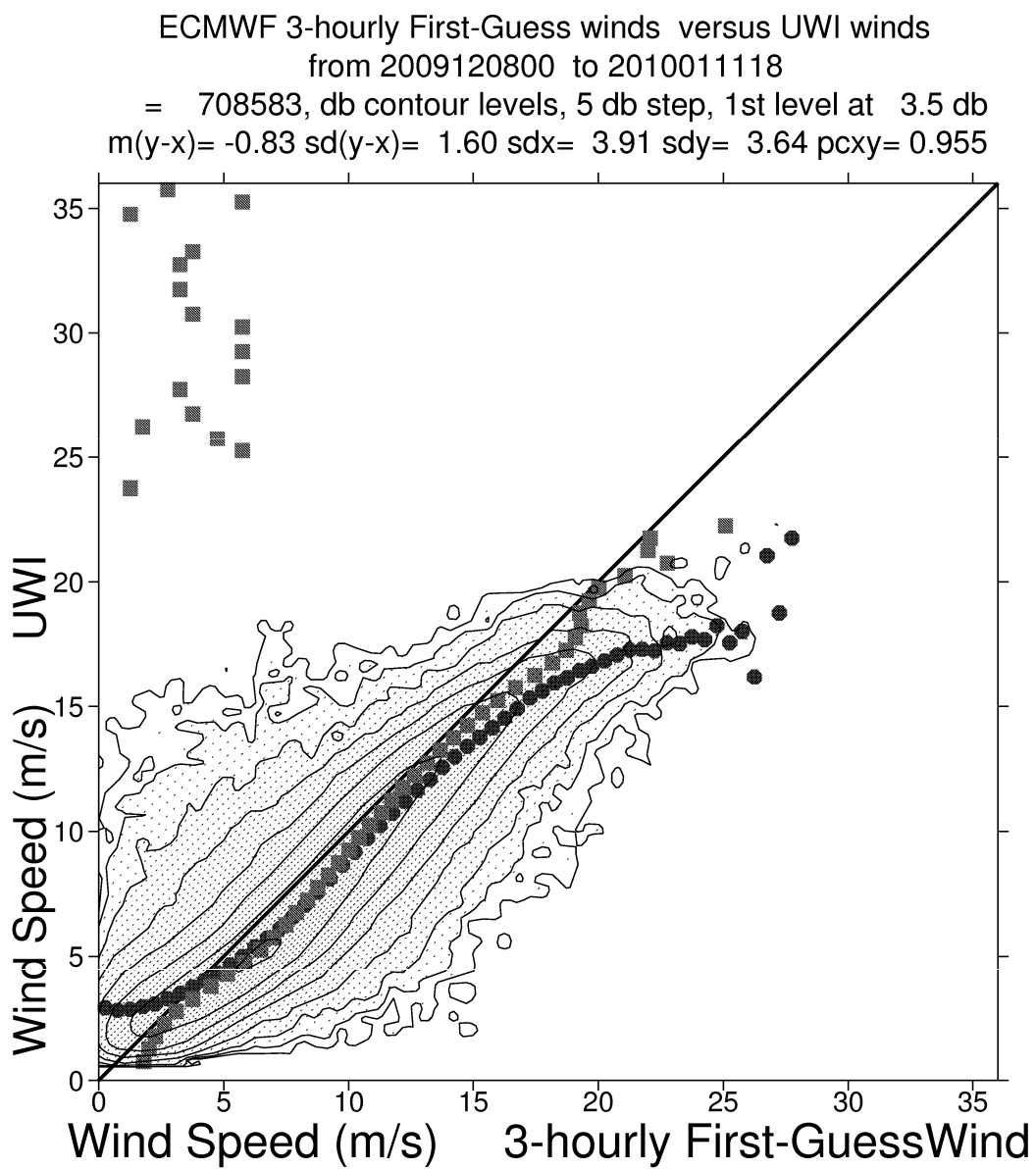


Figure 13

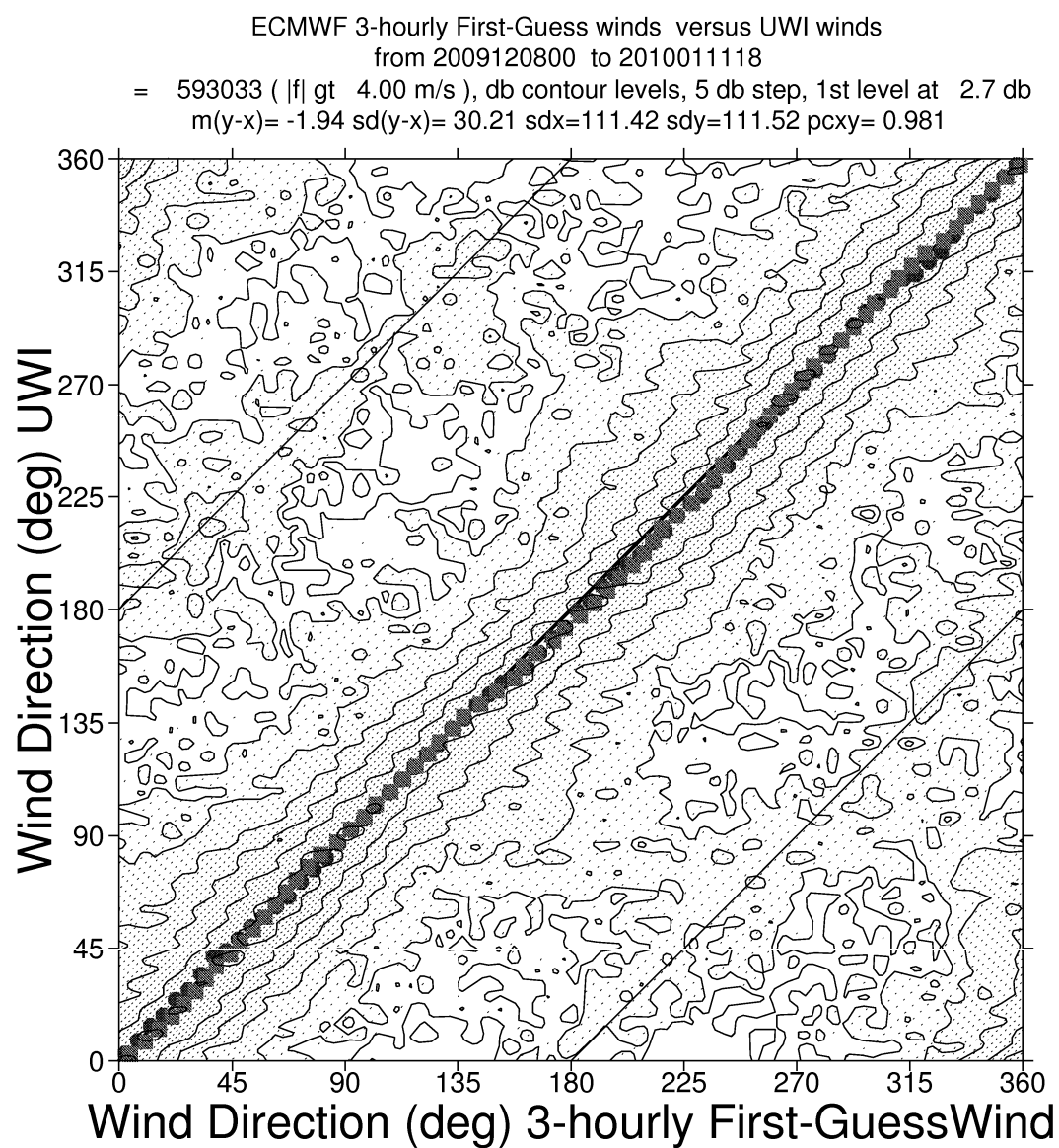


Figure 14

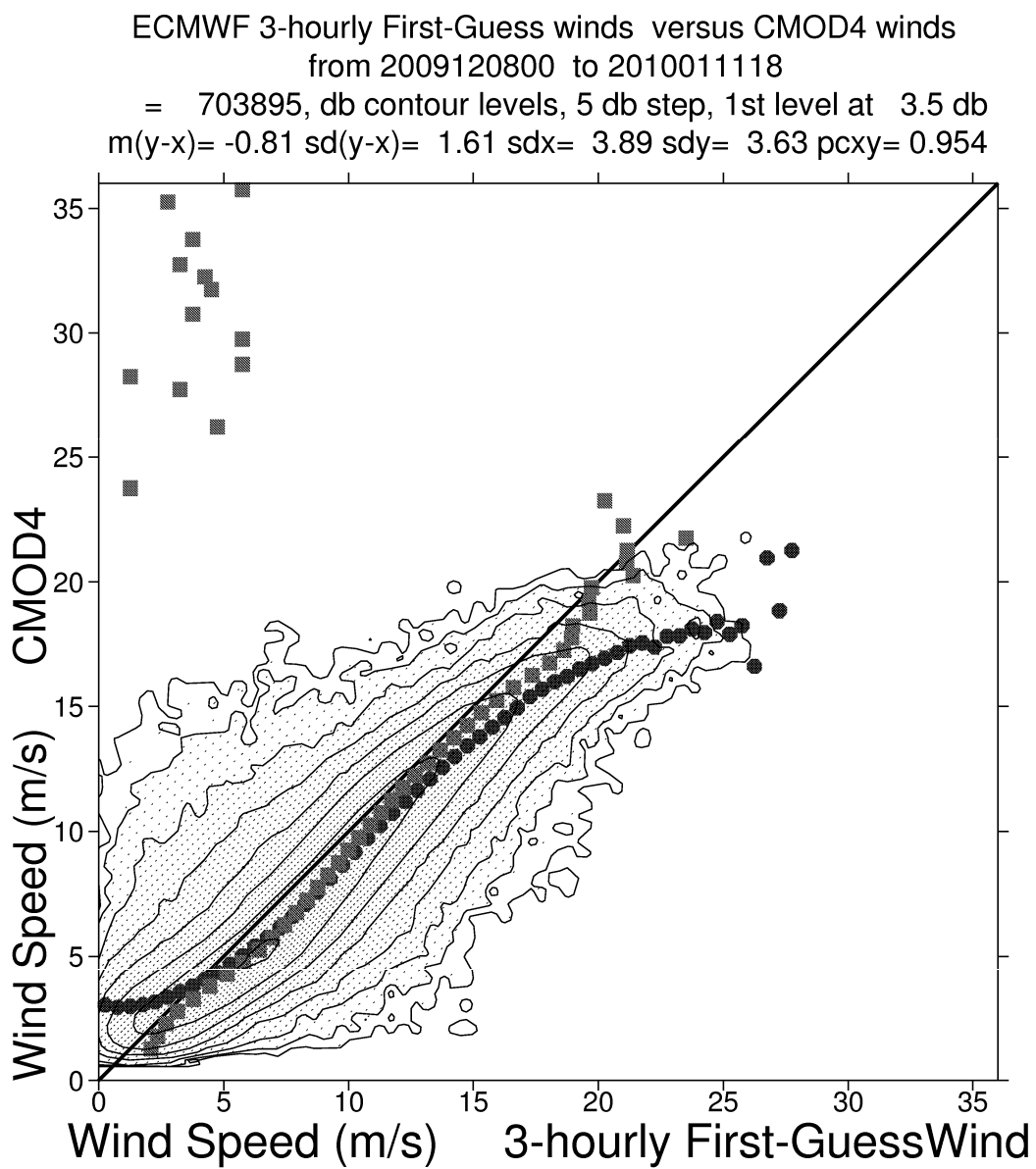


Figure 15

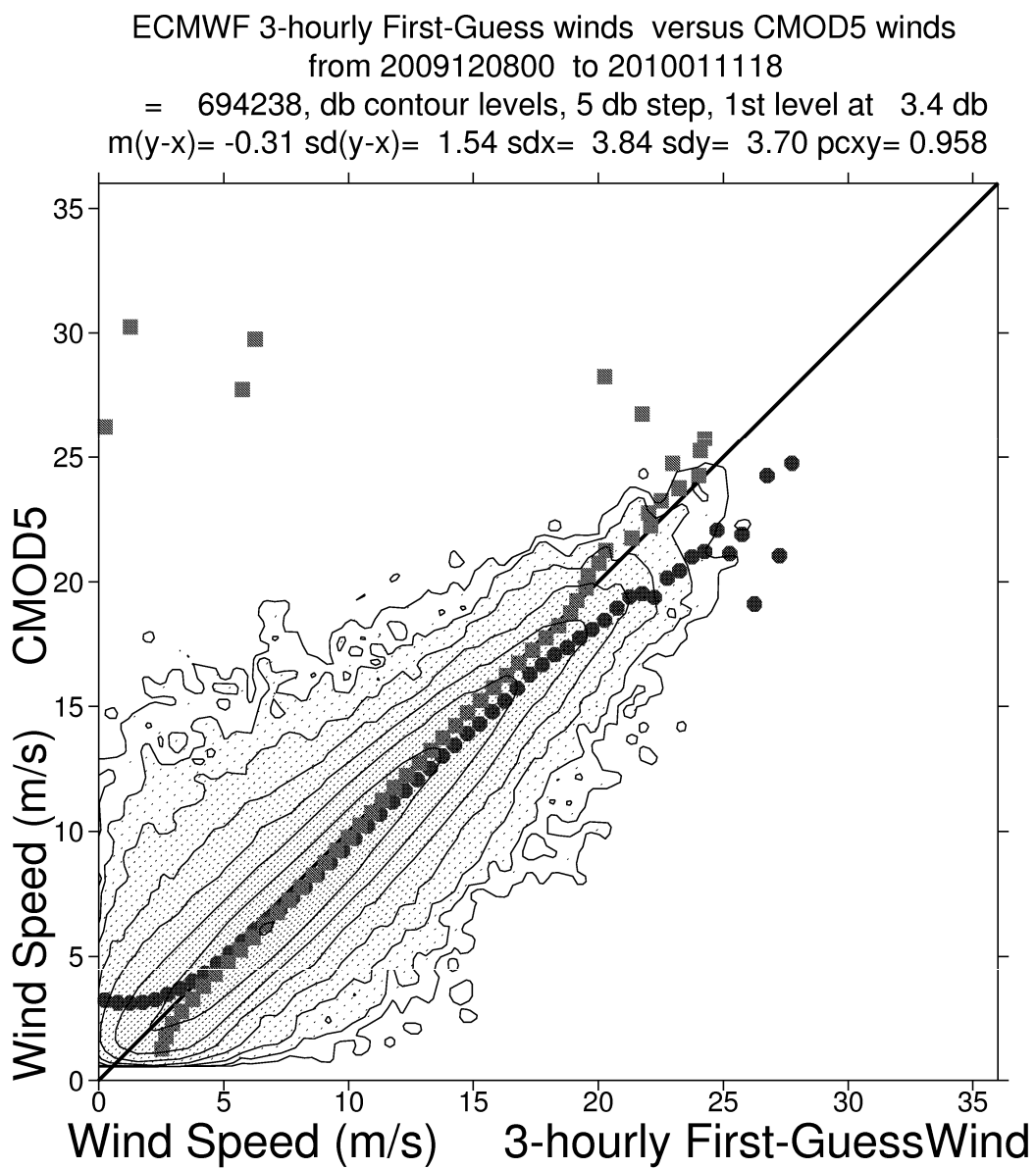


Figure 16